Level statistics and localization transitions of Lévy matrices

E. Tarquini^{1,2,3}, G. Biroli², and M. Tarzia¹

¹ LPTMC, CNRS-UMR 7600, Université Pierre et Marie Curie, boîte 121, 75252 Paris cédex 05, France ² Institut de physique théorique, Université Paris Saclay, CEA, CNRS, F-91191 Gif-sur-Yvette, France ³ Université Paris-Sud, 91405-ORSAY, France

This work provide a thorough study of Lévy or heavy-tailed random matrices (LM). By analysing the self-consistent equation on the probability distribution of the diagonal elements of the resolvent we establish the equation determining the localisation transition and obtain the phase diagram of LMs. Using arguments based on super-symmetric field theory and Dyson Brownian motion we show that the eigenvalue statistics is the same one of the Gaussian Orthogonal Ensemble in the whole delocalised phase and is Poisson in the localised phase. Our numerics confirms these findings, valid in the limit of infinitely large LMs, but also reveals that the characteristic scale governing finite size effects diverges much faster than a power law approaching the transition and is already very large far from it. This leads to a very wide cross-over region in which the system looks as if it were in a mixed phase. Our results, together with the ones obtained previously, provide now a complete theory of Lévy matrices.

Since the well-known pioneering applications of Gaussian random matrices to nuclear spectra, Random Matrix Theory (RMT) found successful applications in many areas of physics [1] and also in other research fields such as wireless communications [2], financial risk [3] and biology [4]. The reason for such remarkable versatility is that RMT provides universal results which are independent on the specific probability distribution of the random matrices: only a few features that determine the universality class matter. The most commonly studied RMs belong to the Gaussian ensembles [1]. They have been analysed in great depth taking advantage of the symmetry under the orthogonal (or unitary/symplectic) group of the probability distribution. As an example of universality, $N \times N$ real symmetric RMs, although they belong to the Gaussian Orthogonal Ensemble (GOE) only if the elements are Gaussian variables, display a GOE-like level statistics also when the distribution of the elements is not Gaussian, provided that it decreases fast enough to infinity [1, 5, 6].

There exists however a large set of matrices that fall out of the universality classes based on the Gaussian paradigm [1]. These are obtained when the entries are heavy-tailed i.i.d. random variables (i.e. with infinite variance). The reference case for this different universality class corresponds to entries that are Lévy distributed. This is the natural generalisation of the Gaussian case since the limiting distribution of the sum of a large number of heavy-tailed i.i.d. random variables is indeed a Lévy distribution, as is the Gaussian distribution for nonheavy tailed random variables. Understanding the statistical spectral properties of these, so called, Lévy matrices (LMs) is an exciting problem from the mathematical and the physical sides [1, 2, 8, 10–14]. They represent a new (and very broad) universality class, with different and somehow unexpected properties with respect to the Gaussian case. Actually, a huge variety of distributions in physics and in other disciplines exhibit powerlaw behavior. Accordingly, LMs appear in several contexts: in models of spin-glasses with dipolar RKKY interactions [15], in disordered electronic systems [16], in portfolio optimization [17] and in the study of correlations in big data sets [18], just to cite a few.

Contrary to the Gaussian case, the theory of random LMs is not yet well-established. They have been introduced in the pioneering work [1] and further studied in [2, 8, 10-14. By now, the behaviour of their density of states has been well understood (even rigorously) [1, 2, 8, 10]. Instead, on finer observables, such as level and eigenfunction statistics, there are scarcer and even conflicting results. This is probably due to the fact that the behaviour of LMs is richer, and hence more difficult to understand, than the one of GOE matrices. For instance, a mobility edge separating high energy localized states from low energy extended states appears within their spectrum [1]. It was also argued that they display a new intermediate mixed phase, characterized by a non-universal level statistics. Although some aspects of the scenario put forward in [1] are in contradiction with recent rigorous results [13], such mixed phase could indeed exist and actually be related to the one recently observed in the Anderson model on the Bethe lattice [9, 19]. It may be the simplest case of the non-ergodic delocalised phase advocated for quantum many body disordered systems in [21].

In the following we focus on $N \times N$ real symmetric matrices \mathcal{H} with entries $h_{ij} = h_{ji}$ distributed independently according to a law, $P(h_{ij}) = N^{1/\mu} f(N^{1/\mu} h_{ij})$, characterized by heavy tails:

$$P(h_{ij}) \simeq \frac{1}{2N|h_{ij}|^{1+\mu}} , |h_{ij}| \to \infty ; \mu < 2.$$

The specific form of f(x) does not matter. For concreteness in numerical applications we will focus on a Student distribution with exponent $1 + \mu$ and symmetric entries, f(x) = f(-x). The scaling of the entries with N is such that almost all eigenvalues are O(1) for $N \to \infty$.

The first issue we address is determining the localization-delocalization transition line $E^*(\mu)$ in the $E-\mu$ plane. In order to do so, we focus on the statistics of the diagonal elements of the resolvent matrix $\mathcal{G} = [(E-i\eta)\mathcal{I}-\mathcal{H}]^{-1}$, which allows one to compute in the $\eta \to 0^+$ limit spectral properties of \mathcal{H} such as the global density of states $\rho(E) = (1/N) \sum_{n=1}^N \delta(E-\lambda_n) = \lim_{\eta \to 0^+} (1/N\pi) \sum_{i=1}^N \Im G_{ii}$ and the average Inverse Participation Ratio (IPR) $\langle \Upsilon_{2,n} \rangle = \langle \sum_{i=1}^N |\langle i|n \rangle|^4 \rangle = \lim_{\eta \to 0^+} (1/N) \sum_{i=1}^N \eta |G_{ii}|^2$. As shown in [1] (see also [2, 8, 10]), the G_{ii} s satisfy in the large-N limit the equation:

$$G_{ii}^{-1} = E - i\eta - \sum_{i=1}^{N} h_{ij}^2 G_{jj}$$
 (1)

Since the G_{ii} s are random variables, this naturally defines a self-consistent equation on their probability distribution Q(G), whose analysis yields the results on the density of states obtained in [1, 2]: For $\mu < 2$, $\rho(E)$ is a μ -dependent symmetric distribution with support on the whole real axis and fat tails with exponent $1 + \mu$ (the semicircle law is recovered for $\mu > 2$ only). There are several complementary ways to obtain the localisation transition from the statistics of the G_{ii} s. We have followed the one more likely to receive a rigorous treatment, as it was shown for the Anderson transition on the Bethe lattice [22]. It consists in studying the stability of the localised phase, checking whether adding a small imaginary part to G_{ii} is an unstable perturbation [6]. Such stability is governed by an eigenvalue equation for the same integral operator found in [1], whose analysis can be considerably simplified, as shown in the EPAPS [32], and boils down to the following closed equation for the mobility edge, which is one of the main results of this work:

$$K_{\mu}^{2} \left(s_{\mu}^{2} - s_{1/2}^{2} \right) |\ell(E^{\star})|^{2} - 2s_{\mu}K_{\mu} \Re \ell(E^{\star}) + 1 = 0,$$
 (2)

where $K_{\mu} = \Gamma(1/2 - \mu/2)^2/2$, $s_{\mu} = \sin(\pi \mu/2)$ and $\ell(E) = \int_0^{+\infty} k^{\mu-1} \hat{L}_{\mu/2}^{C(E),\beta(E)}(k) \, e^{ikE} \, \mathrm{d}k/\pi$. The function $\hat{L}_{\mu/2}^{C(E),\beta(E)}(k)$ is the Fourier transform of the probability distribution of the real part of the self-energy, that previous works have shown to be a Lévy stable distribution with exponent $1 + \mu/2$ and parameters C(E) and $\beta(E)$ determined self-consistently [1, 2, 8]. This equation has a solution for $\mu \in (0,1)$ only. For $\mu \to 1$ we find that $E^{\star}(\mu)$ diverges as $1/(1-\mu)$. In fig. 1 we show the numerical solution of Eq. (2) for several values of μ (we only consider E>0 since the spectral properties are symmetric around zero). This quantitative phase diagram is in agreement with the sketch of [1] (the difference for $\mu \to 0$ is just due to a different normalisation of h_{ij}) and the numerics of [10] (except for $\mu > 1$ where the results were likely inaccurate due to the very large values of E that had to be explored).

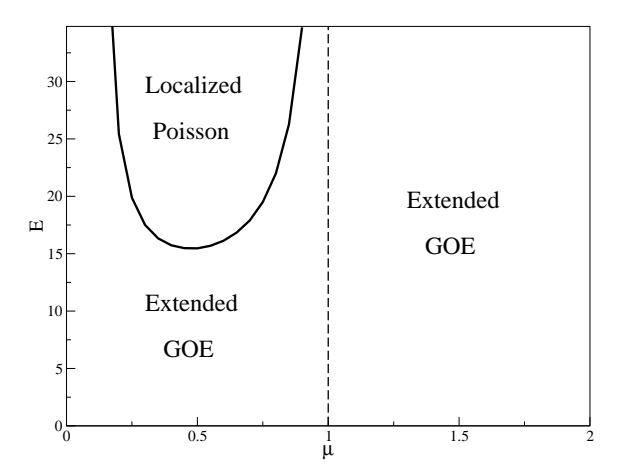


FIG. 1. Phase diagram of LMs in the μ -E plane.

We now address more subtle issues related to the level and eigenfunction statistics. We present first two analytical arguments which show that the statistics is GOE in the whole delocalised phase and Poisson in the localized phase for $N \to \infty$. The former is based on the supersymmetric zero-dimensional field theory introduced for random GOE matrices [24]. The starting point is the field theory $Z = \int \prod_i \mathrm{d}\Phi_i e^{S[\Phi_i]}$, with the action:

$$S = \frac{i}{2} \left(\sum_{l,m} \Phi_l^{\dagger} \mathcal{L}(E\delta_{lm} - h_{lm}) \Phi_m + \sum_l \Phi_l^{\dagger} \Phi_l \frac{r + i0^+}{N} \right)$$

The field Φ_i is a eight-component super-vector $(\Phi_i^{(1)}, \Phi_i^{(2)}) = (S_i^a, S_i^b, \chi_i, \chi_i^*, P_i^a, P_i^b, \eta_i, \eta_i^*)$, where each of the four component super-vector $\Phi_i^{(1,2)}$ is formed by two real and two Grassman variables. The matrix \mathcal{L} is diagonal with elements (1, 1, 1, 1, -1, -1, -1, -1). The level statistics, in particular the density of states and the correlation between two levels at distance r/2N, can be obtained from correlation functions of the fields [24]. Averaging over the the matrix elements and introducing the function $\rho(\Phi) = \frac{1}{N} \sum_i \delta(\Phi - \Phi_i)$ one can rewrite Z as $\int \mathcal{D}\rho(\Phi)e^{S[\rho]}$ with the action reading

$$S = \frac{i}{2} N E \int d\Phi \rho(\Phi) \Phi^{\dagger} \mathcal{L} \Phi + \frac{i}{2} (r + i0^{+}) \int d\Phi \rho(\Phi) \Phi^{\dagger} \Phi$$
$$- N \int d\Phi \rho(\Phi) \log \rho(\Phi) + \frac{i}{2} N \int d\Phi d\Psi \rho(\Phi) C(\Phi^{\dagger} \mathcal{L} \Psi) \rho(\Psi)$$

where $C(y) = \int \frac{\mathrm{d}x}{x^{1+\mu}} [\exp(-ixy) - 1]$. Since the second term is sub-leading compared to the other three that are O(N), one can neglect it at first and perform a saddle-point. Before discussing the corresponding equation it is useful to remark that $\rho(\Phi)$ has a particularly illuminating expression (easy to obtain by direct integration before disorder average) [25]:

$$\rho(\Phi) = \int d\Sigma R(\Sigma) \exp\left(\frac{i}{2}\Phi^{\dagger}\mathcal{L}\Phi(E - \Re\Sigma) + \frac{1}{2}\Phi^{\dagger}\Phi\Im\Sigma\right)$$

where $R(\Sigma)$ is the distribution of the local self-energy. By plugging this expression into the saddle-point equation one finds that $R(\Sigma)$ is a complex Levy-distribution with parameters satisfying the self-consistent equation rigorously proven in [2]. Note that the saddle point equation is invariant under the symmetry $\Phi \to \mathcal{T}\Phi$ where the super matrix \mathcal{T} verifies the equation $\mathcal{T}^{\dagger}\mathcal{L}\mathcal{T}=1$. Thus given a solution $\rho(\Phi)$, $\rho_{\mathcal{T}}(\Phi) = \rho(\mathcal{T}\Phi)$ is also a solution. The localisation transition corresponds to the breaking of this symmetry [24, 26]: in the localised phase the typical value of the imaginary part of the self-energy is zero, whereas it is finite in the delocalised phase. In consequence, in the former case $\rho(\Phi)$ is a function of $\Phi^{\dagger}\mathcal{L}\Phi$ only, invariant under the symmetry generated by \mathcal{T} , whereas in the latter it depends also on $\Phi^{\dagger}\Phi$. Since this dependence breaks the symmetry there is a manifold of solutions $\rho_{\mathcal{T}}(\Phi)$. It is the integration over this manifold that leads to GOE statistics for the level correlations. The derivation is identical to the one presented in [26] since the only term in the action that depends on \mathcal{T} , i.e. that breaks the symmetry, is the r-one as it happens for Erdos-Renyi graphs [27] and GOE RMs [24]. In the localised phase, the saddle point solution is instead unique. Therefore no integration over \mathcal{T} has to be performed and this leads to uncorrelated levels, i.e. Poisson statistics [26].

Let us now turn to the other analytical argument, which is very straightforward but limited to $\mu > 1$ only. Taking inspiration from the recent mathematical breakthrough on RMT [5], we slightly modify the distribution $P(h_{ij})$ into $(1 - \epsilon)P(h_{ij}) + \epsilon N^{1/\mu}W(N^{1/\mu}h_{ij})$ where W(x) is a Gaussian distribution with unit variance. This is equivalent to modify \mathcal{H} into $\mathcal{H}_{\epsilon} = (1 - \epsilon)\mathcal{H} + \epsilon \mathcal{W}$ where \mathcal{H} is a LM and W a very small GOE matrix whose elements have exactly the same scaling with N than the ones of \mathcal{H} . Since this change does not alter the fat tails of the matrix elements, one naturally expects \mathcal{H}_{ϵ} and \mathcal{H} to be in the same universality class for any $\epsilon < 1$ and in particular for $\epsilon \to 0$. The statistics of the modified LM—and, by the previous argument, of \mathcal{H} —can be obtained using the Dyson Brownian Motion (DBM): \mathcal{H}_{ϵ} can be interpreted, in the basis that diagonalises \mathcal{H} , as a diagonal matrix to which an infinite number of infinitesimal GOE matrices, adding up to give W, have been added. The probability of the eigenvalues of \mathcal{H}_{ϵ} is therefore given by the DBM starting from the eigenvalues of \mathcal{H} , and evolving over a fictive time of the order $N^{-1/\mu}$. Recent rigorous results, that can be also obtained heuristically in a simple way [5, 31], guarantee that the DBM has enough "time" to reach its stationary distribution, which is the GOE distribution, if $N^{-1/\mu} \gg N^{-1}$ and the typical level spacing of \mathcal{H} is O(1/N)-a very reasonable assumption that agrees well with numerics. This implies that for $\mu > 1$ the level statistics of the modified LM, and hence of the original LM too, is indeed GOE-like in the bulk of the spectrum [30]. A similar argument also applies to the eigenfunctions [31, 33].

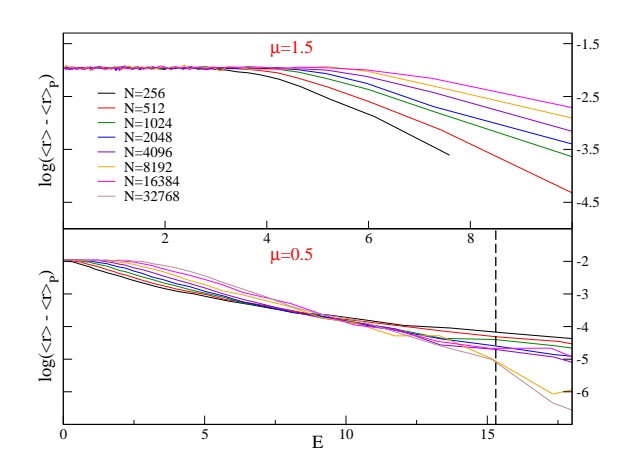


FIG. 2. $\ln[(\langle r \rangle - \langle r \rangle_P)/(\langle r \rangle_{GOE} - \langle r \rangle_P)]$ as a function of E for different system sizes and for $\mu = 1.5$ (top) and $\mu = 0.5$ (bottom). The dashed line represents the position of the mobility edge, $E^* \simeq 15.4$.

We now present several numerical results with the aim of backing up our previous analytical arguments and also of studying the behaviour of large but finite LMs. In applications N is never truly infinite, actually in several cases it can be just a few thousands. Thus, it is of paramount importance to study finite size effects and determining the characteristic value of N above which the $N \to \infty$ limit is recovered. We performed exact diagonalization of LMs for several system sizes $N=2^n$, from n=8 to n=15 and averaging over 2^{22-n} realizations of the disorder. We have resolved the energy spectrum in 64 small intervals ν , centered around the energies $E_{\nu} = \langle \lambda_n \rangle_{n \in \nu}$, and analysed the statistics of eigenvalues and eigenfunctions in each one of them. We have focused on several observables that display different universal behaviours in the GOE and Poisson regimes: The first probe, introduced in [28], is the ratio of adjacent gaps $r_n =$ $\min\{\delta_n, \delta_{n+1}\}/\max\{\delta_n, \delta_{n+1}\}\$ where $\delta_n = \lambda_{n+1} - \lambda_n \geq 0$ denotes the level spacings between neighboring eigenvalues. It has different universal distributions in the GOE and Poisson cases encoding respectively the repulsion or the independence of levels. The second one is the overlap between eigenvectors corresponding to subsequent eigenvalues, defined as $q_n = \sum_{i=1}^N |\langle i|n\rangle| |\langle i|n+1\rangle|$. Its typical value $q_{\nu}^{typ} = e^{\langle \ln q_n \rangle_{n \in \nu}}$ allows to make the difference between the localised phase, in which subsequent eigenvectors do not overlap $(q^{typ} = 0)$, and the delocalised-GOE one in which they do $(q^{typ} = 2/\pi)$. Finally, the wave-function support set, recently introduced in [29], is defined for an eigenvector n with sites ordered according to $|\langle i|n\rangle| > |\langle i+1|n\rangle|$ as the sets of sites $i < S_{\epsilon}^{(n)}$ such that $\sum_{i=1}^{S_{\epsilon}^{(n)}} |\langle i|n\rangle|^2 \le 1 - \epsilon < \sum_{i=1}^{S_{\epsilon}^{(n)}+1} |\langle i|n\rangle|^2$. The scaling of $S_{\epsilon}^{(n)}(N)$ for $N \to \infty$ and ϵ arbitrary small but finite allows to discriminate between localised and extended phase. The analysis of all these probes clearly

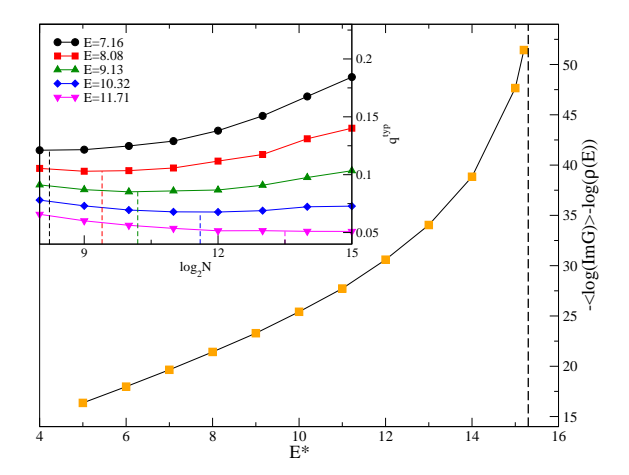


FIG. 3. Main panel: $\log N'_m(E)$ as a function of E for $\mu = 0.5$. Inset: q_{typ} as a function of N for different energies and $\mu = 0.5$, showing the position of $N_m(E)$.

shows that for $\mu > 1$ the statistics is GOE in the limit of large N, in agreement with our previous arguments (and also with the rigorous results on the delocalised nature of wave-functions [13]). As an example we show in the top panel of fig. 2 the behaviour of the average value of r_n for $\mu = 1.5$. It clearly converges in the limit $N \to \infty$ and for any energy E to the value $\langle r_n \rangle_{GOE} \simeq 0.53$ characteristic of GOE statistics. All other probes show a similar convergence to the values expected for GOE statistics (see EPAPS [32] for the corresponding plots). This is no longer true for $\mu < 1$, where the situation is more involved. In the lower panel of fig. 2 we show again the behaviour of the average of r_n but now for $\mu = 0.5$. For small and large energies we find the values $\langle r \rangle_{GOE} \simeq 0.53$ and $\langle r \rangle_P \simeq 0.39$ corresponding respectively to GOE and Poisson statistics. Moreover, the curves corresponding to different values of N seem to cross much before the localization transition, that our previous analytical results located at $E^{\star} \simeq 15.4$ for $\mu = 0.5$. If this were representative of the truly asymptotic large-N behaviour then it would possibly signal the existence of a mixed phase which could be delocalized but non-ergodic, i.e. not displaying GOE statistics. However, analysing carefully the data-thanks to the large number of samples used to average over the disorder-we find that the crossing point is in fact very slowly drifting towards higher energies as N is increased. The same behaviour is found for all the probes we studied. As an example, in the inset of fig. 3 we plot q_{ν}^{typ} as a function of the system size for energies belonging to the crossing region. This indeed shows that q_{typ} is a non-monotonic function of N. We can then define a characteristic matrix size, $N_m(E)$, such that for $N \ll N_m(E)$ the statistics appears to be intermediate between Poisson and GOE (see EPAPS [32]), whereas for $N \gg N_m(E)$ it tends again toward GOE.

The existence of a cross-over size can be understood from

the properties of the distribution Q(G). What characterises the delocalised phase is that, at any site i, the imaginary part of G_{ii} receives an infinitesimal contribution from an infinite number of eigenfunctions. This leads to a typical value of G_{ii} (defined as $\Im G_{ii}^{typ} = e^{\langle \log \Im G_{ii} \rangle}$) which is finite for $N \to \infty$ and $\eta \to 0$. Instead, $\Im G_{ii}^{typ} = 0$ in the localised phase. Approaching the transition from the delocalized side, $\Im G_{ii}^{typ}$ becomes extremely small. Thus, one needs to take large enough systems in order to realize that it is different from zero, and hence that the system is in the delocalised and GOE-like phase. The argument, which is based on the interpretation of $\Im G_{ii}$ as the local density of states, is as follows. The number of states per unit of energy close to E is $N\rho(E)$. This number, multiplied by the typical value of the local density of states, has to be larger than one in order to be in a regime representative of the large-N limit. This defines the cross-over scale $N'_m(E) \propto 1/(\Im G_{ii}^{typ} \rho(E))$. We have compared numerically $\ln N_m'(E)$ and $\ln N_m(E)$ and found that they are indeed proportional (see the EPAPS [32] for a plot), thus showing that our argument correctly captures the origin of the finite size effects. We plot the cross-over scale (actually $N_m'(E)$) as a function of E in fig. 3 for $\mu = 0.5$: it diverges very fast approaching $E^{\star}(\mu)$. A good fit is provided by an essential singularity. These results therefore unveil what is the mechanism responsible for the non-GOE statistics observed in a wide regime before the localisation transition for finite LMs.

In conclusion, we have presented a thorough analysis of the eigenvalues and eigenvectors statistics of random Lévy Matrices. We have shown that the localisation and the level statistics transitions coincide but also unveiled the existence of a cross-over scale which is very large even far from the transition. Thus, many practical cases are expected to be in the $N \ll N_m(E)$ regime. In consequence, the mixed behaviour proposed in [1] will be often present in practice even though it is absent in the large-N limit. Our work, together with the results obtained previously, provides now a complete theory of LMs. There are severals directions worth pursuing more. It would be interesting to determine analytically the form of the divergence of $N_m(E)$. On the basis of our numerics and in analogy with previous works [24, 26, 27] we expect $N_m(E) \propto e^{c/(E^*-E)^a}$. Most probably, the emergence of the cross-over scale producing an apparent mixed phase takes place in several other related situations (e.g. [19]) that are therefore to be re-analysed. Finally, our results shows a guideline for mathematicians working on RMT. Thanks to the recent advances in the mathematical analysis of random matrices [5] and localisation phenomena [22] our findings are likely to be rigorously proven in a not too distant future.

We thank G. Ben Arous, J.-P. Bouchaud, L. Erdös, S. Warzel for helpful discussions and acknowledge support from the ERC grant NPRGGLASS. Part of this work was done at the ESI.

- [1] For reviews on random matrix models and techniques see, e.g., M.L. Mehta, Random Matrices, 3rd Edition, (Elsevier-Academic Press, 2004); S.N. Majumdar, Random Matrices, the Ulam Problem, Directed Polymers & Growth Models, and Sequence Matching, Les Houches lecture notes for the summer school on Complex Systems (Les Houches, 2006); T. Guhr, A. Mueller-Groeling, H. A. Weidenmueller, Phys. Rep. 299 189 (1998).
- [2] E. Telatar, European Transactions on Telecommunications 10, **585** (1999).
- [3] L. Laloux, P. Cizeau, J.-P. Bouchaud, and M. Potters, Phys. Rev. Lett. 83, 1467 (1999).
- [4] F. Luo, P.K. Srimani, J. Zhou, Handbook of Data Intensive Computing 711 (2011).
- [5] L. Erdös, A. Knowles, H.-T. Yau, J. Yin, Electronic J. of Probability, 18, 1 (2013).
- [6] T. Tao and V. Vu, Acta Math, 206 127 (2011).
- [7] P. Cizeau and J.-P. Bouchaud, Phys. Rev. E 50, 1810 (1994).
- [8] Z. Burda, J. Jurkiewicz, M.A. Nowak, G. Papp, and I. Zahed, Phys. Rev. E 75, 051126 (2007).
- [9] F.L. Metz, I. Neri, and D Bollé, Phys. Rev. E 82, 031135 (2010).
- [10] G. Ben Arous and A. Guionnet, Comm. in Math. Phys. 278 715 (2008).
- [11] G. Biroli, J.-P. Bouchaud, M. Potters, EPL 78 78 (2007).
- [12] A. Auffinger, G. Ben Arous, S. Péché, Annales de l'IHP
 Probabilités et Statistiques, 45 589 (2009).
- [13] C. Bordenave and A. Guionnet, Probab. Theory and Relat. Fields, 157 885 (2013).
- [14] S. Majumdar, G. Schehr, D. Villamaina, and P. Vivo, J. Phys. A: Math. Gen. 46, 022001 (2013).
- [15] P. Cizeau and J.-P. Bouchaud, J. Phys. A: Math. Gen. 26, L187 (1993).
- [16] L.S. Levitov, Europhys. Lett. 9, 83 (1989).
- [17] S. Galluccio, J.-P. Bouchaud, and M. Potters, Physica A

- **259**, 449 (1998).
- [18] M. Politi, E. Scalas, D. Fulger, and G. Germano, Eur. Phys. J. B 73, 13 (2010).
- [19] G. Biroli, A.C. Ribeiro Teixeira, and M. Tarzia, arXiv: 1211.7334.
- [20] A. De Luca, B. Altshuler, V.E. Kravtsov, A. Scardicchio Phys. Rev. Lett 113 046806 (2014).
- [21] B.L. Altshuler et al., Phys. Rev. Lett. 78, 2803 (1997).
- [22] M. Aizenman and S. Warzel, J. of the Europ. Math. Soc. 15 1167 (2013).
- [23] R. Abou-Chacra, P.W. Anderson, and D.J. Thouless, J. Phys. C: Solid St. Phys. 6, 1734 (1973).
- [24] K. Efetov, Supersymmetry in Disorder and Chaos, Cambridge Univ. Press 1997.
- [25] A.D. Mirlin, and Y.V. Fyodorov, J. Phys. I France 2, 1571 (1992).
- [26] A.D. Mirlin and Y.V. Fyodorov Nucl. Phys. B 366 507 (1991).
- [27] Y.V. Fyodorov and A.D. Mirlin Phys. Rev. Lett. 67 2049 (1991).
- [28] V. Oganesyan and D. Huse, Phys. Rev. B 75, 155111 (2007).
- [29] A. De Luca, V.E. Kravtsov, B. L. Altshuler, and A. Scardicchio, arXiv:1401.0019.
- [30] For the edge the result is different: one needs $\mu > 4$ [11, 12]) as a variant of this argument would also suggest.
- [31] R. Allez, J.-P. Bouchaud, and A. Guionnet, Phys. Rev. Lett. 109, 094102 (2012).
- [32] See the EPAPS, which includes Refs [34–39]
- [33] P. Bourgade and H.T. Yau, arXiv:1312.1301.
- [34] B. Derrida and H. Spohn, J. Stat. Phys. **51**, 817 (1988).
- [35] B. Derrida, Phys. Rev. Lett. 45, 79 (1980).
- [36] V. Bapst, J. Math. Phys. 55, 092101 (2014).
- [37] Y.Y. Atas, E. Bogomolny, O. Giraud, and P. Vivo, J. Phys. A: Math. Gen. 46, 355204 (2103).
- [38] K. Janzen, A. Engel, and M. Mézard, Europhys. Lett. 89, 67002 (2010).
- [39] M. Mézard and G. Parisi, Eur. Phys. J. B 20 (2001), 217.

EPAPS

In this supplementary material we provide more details and results related to several points discussed in the main text. For definiteness we shall consider $N \times N$ real symmetric (Wigner) Lévy Matrices \mathcal{H} with entries $h_{ij} = h_{ji}$ distributed independently according to a student distribution with exponent $1 + \mu$ and typical value of order $N^{-1/\mu}$:

$$P(h_{ij}) = \theta \left(|h_{ij}| > (N\mu)^{-1/\mu} \right) \frac{1}{2N|h_{ij}|^{1+\mu}}.$$
 (3)

COMPUTATION OF THE MOBILITY EDGE

In order to determine the position of the mobility edge, it is convenient to introduce the self-energy $\Sigma_i = E - i\eta - G_{ii}^{-1} = S_i + i\Delta_i$, and linearize the recursive equations for the diagonal elements of the resolvent matrix [Eq. (1) of the main text] with respect to their imaginary part in the limit $\eta \to 0^+$:

$$S_i = \sum_{j=1}^{N} h_{ij}^2 \Re G_{jj} = \sum_{j=1}^{N} \frac{h_{ij}^2}{E - S_j},$$
(4a)

$$\Delta_i = \sum_{j=1}^N h_{ij}^2 \Im G_{jj} = \sum_{j=1}^N \frac{h_{ij}^2}{(E - S_j)^2} \, \Delta_j \,. \tag{4b}$$

The recursion relation (4a) for the real part of the self-energy totally decouples from the equation (4b) for its imaginary part. The marginal probability distribution of the real part can thus be computed using the generalized central limit theorem. The matrix elements h_{ij} and the terms G_{jj} are uncorrelated in the $N \to \infty$ limit. Since the variance of the entries is infinite for $\mu < 2$, by virtue of the generalized central limit theorem the probability distribution of the variable S tends, for $N \to \infty$, to a Lévy stable distribution, $L_{\mu/2}^{C(E),\beta(E)}(S)$, with stability index $\mu/2$, and "effective range" C(E) and "asymmetry parameter" $\beta(E)$ given by:

$$C = \frac{\Gamma\left(1 - \frac{\mu}{2}\right)\cos\left(\frac{\pi\mu}{4}\right)}{\mu} \frac{1}{N} \sum_{j=1}^{N} |\text{Re}G_{jj}|^{\frac{\mu}{2}} ,$$

$$\beta = \frac{\frac{1}{N} \sum_{j=1}^{N} |\text{Re}G_{jj}|^{\frac{\mu}{2}} \sin(\text{Re}G_{jj})}{\frac{1}{N} \sum_{j=1}^{N} |\text{Re}G_{jj}|^{\frac{\mu}{2}}} .$$
(5)

In the $N \to \infty$ limit the diagonal elements of the resolvent become independent and identically distributed. We can therefore replace the sums in the r.h.s. of Eqs. (5) by integrals over the marginal probability distribution $\tilde{Q}_R(\text{Re}G)$. In the limit of vanishing imaginary part, one has that $S_i = E - 1/\text{Re}G_{ii}$. Hence by changing variable one has:

$$\tilde{Q}_R(\mathrm{Re}G)\,\mathrm{dRe}G = L_{\mu/2}^{C(E),\beta(E)}\left(E - \frac{1}{\mathrm{Re}G}\right)\frac{\mathrm{dRe}G}{|\mathrm{Re}G|^2}\,.$$

As a consequence, Eq. (5) can be written as a set of two coupled self-consistent equation for the parameters C(E) and $\beta(E)$ [1, 2], which can be solved numerically with a reasonably high degree of accuracy.

$$C(E) = \frac{\Gamma\left(1 - \frac{\mu}{2}\right)\cos\left(\frac{\pi\mu}{4}\right)}{\mu} \int_{-\infty}^{+\infty} L_{\mu/2}^{C(E),\beta(E)}(S) |E - S|^{-\frac{\mu}{2}} dS, \qquad (6a)$$

$$\beta(E) = \frac{\int_{-\infty}^{+\infty} L_{\mu/2}^{C(E),\beta(E)}(S) \operatorname{sign}(E - S) |E - S|^{-\frac{\mu}{2}} dS}{\int_{-\infty}^{+\infty} L_{\mu/2}^{C(E),\beta(E)}(S) |E - S|^{-\frac{\mu}{2}} dS}.$$
 (6b)

Focusing on the recursive equation (4b) for the imaginary part of the self-energy one realizes that it satisfies the same recursive equation as the partition function of directed polymers in random media (DPRM) [3] in presence of quenched (correlated) bond disorder $e^{-\epsilon_{ij}} = h_{ij}^2/(E - S_j)^2$. One can therefore use the results established in this context, and telescope Eq. (4b) as:

$$\Delta_{i_1} = \sum_{\mathcal{P}} \left(\prod_{(i_{n+1}, i_n)} \frac{h_{i_n, i_{n+1}}^2}{(E - S_{i_{n+1}})^2} \right) \Delta_{i_R} , \qquad (7)$$

where $\mathcal{P} = (i_1, i_2, \dots, i_R)$ denotes all the directed paths of length R originating from the site i_1 , and (i_{n+1}, i_n) are all the edges belonging to the path. The sum in (7) is thus over an exponential number of paths, $(N-1)!/(N-R-1)! \sim N^R$. In the large R limit, two cases are possible: the sum is dominated either by few paths that give a O(1) contribution, or by an exponential number of paths, each of them giving a very small contribution but such that their sum is O(1). The transition between these two regimes corresponds to the freezing-glass transition (called one-step Replica Symmetry Breaking) of DPRM, akin to the one of the Random Energy Model [3, 4]. In order to determine the transition point, one has to compute the (annealed) replicated free energy of DPRM:

$$\phi(m, E) = \frac{1}{Rm} \log \left(\sum_{\mathcal{P}} \prod_{(i_{n+1}, i_n)} \left| \frac{h_{i_n, i_{n+1}}}{E - S_{i_{n+1}}} \right|^{2m} \right), \tag{8}$$

which gives the behavior of the typical value of Δ_i^m , and impose that $\partial \phi/\partial m|_{m=m^*}=0$. In fact, the glass phase of DPRM corresponds to the Anderson localized regime, where the imaginary part of the self-energy is of order η with probability 1 on (almost) all the sites, except on extremely rare and distant resonances where it is of O(1). Conversely, the ergodic phase of DPs corresponds to the delocalized regime, where Δ_i is of O(1) on all the sites. For the Anderson model on the Bethe lattice the localization transition takes place for m=1/2 and $\phi(m^*)=0$, as it has been rigorously proven in [5, 7] and indirectly found in [6]. It turns out that the this is also the case for Lévy Matrices

Considering the site i_n of a given path, using the recursion relation (4a), one can rewrite the real part of the self-energy as:

$$S_{i_n} = \frac{h_{i_n,i_{n+1}}^2}{E - S_{i_n+1}} + \sum_{i_n'=1}^{N-2} \frac{h_{i_n,i_n'}^2}{E - S_{i_n'}'} \,,$$

where the sum over i'_n runs over all the N-2 neighbors of i_n except the sites i_n and i_{n+1} which belong to the path. As a result, averaging over the quenched disorder the free energy (8) is written in terms of the largest eigenvalue, $\lambda(m, E)$, of the following transfer-matrix integral operator:

$$Z_{i_{n}}(S_{i_{n}}) = (N-2) \int dS_{i_{n+1}} Z_{i_{n+1}}(S_{i_{n+1}}) dh_{i_{n},i_{n+1}} P(h_{i_{n},i_{n+1}}) \prod_{i'_{n}}^{N-2} \left[dh_{i_{n},i'_{n}} P(h_{i_{n},i'_{n}}) dS_{i'_{n}} L_{\mu/2}^{C(E),\beta(E)}(S_{i'_{n}}) \right]$$

$$\times \left| \frac{h_{i_{n},i_{n+1}}}{E - S_{i_{n+1}}} \right|^{2m} \delta \left(S_{i_{n}} - \frac{h_{i_{n},i_{n+1}}^{2}}{E - S_{i_{n+1}}} - \sum_{i'_{n}}^{N-2} \frac{h_{i'_{n}}^{2}}{E - S_{i'_{n}}} \right),$$

$$(9)$$

where the factor N-2 accounts for the number of way one can choose the neighbors i_{n+1} among all the N-1 neighbors of i_n except the site i_{n-1} . For large R one has that $\phi(m, E) \simeq (1/m) \log \lambda(m, E)$. As a consequence, the mobility edge is found at the value of E^* where:

$$\begin{cases} \frac{1}{m} \log \lambda(m, E^*) = 0, \\ \frac{\partial}{\partial m} \left[\frac{1}{m} \log \lambda(m, E^*) \right] = 0. \end{cases}$$

This yields:

$$\begin{cases} \lambda(m, E^*) = 1, \\ \frac{\partial}{\partial m} \lambda(m, E^*) = 0. \end{cases}$$
 (10)

Note that this is equivalent to study the stability of the localized phase by checking whether a small imaginary part vanishes exponentially under iteration, as done in [1, 6] (in this case $\lambda(m, E)$ corresponds to the Lyapunov exponent of the imaginary part of the self-energy and m plays the role of the exponent of the power-law tails of its marginal probability distribution). It is convenient to introduce the variable S via the relation

$$\int \mathrm{d} S \, \delta \left(S - \sum_{i'_n = 1}^{N-2} \frac{h_{i_n, i'_n}^2}{E - S_{i'_n}} \right) = 1 \, .$$

In the thermodynamic limit, $N-2\simeq N-1\simeq N$, it is natural to assume that S has the same stationary distribution of the real part of the self-energy, $L_{\mu/2}^{C(E),\beta(E)}(S)$:

$$\int \prod_{i'_n}^{N-2} \left[dh_{i_n,i'_n} P(h_{i_n,i'_n}) dS_{i'_n} L_{\mu/2}^{C(E),\beta(E)}(S_{i'_n}) \right] \delta \left(S - \sum_{i'_n=1}^{N-2} \frac{h_{i_n,i'_n}^2}{E - S_{i'_n}} \right) \underset{N \to \infty}{\simeq} L_{\mu/2}^{C(E),\beta(E)}(S) .$$

Eq. (9) then becomes:

$$Z(X) = N \int dh \, P(h) \, dS \, L_{\mu/2}^{C(E),\beta(E)}(S) \, dX' Z(X') \, \delta \left(X - S - \frac{h^2}{E - X'} \right) \left| \frac{h}{E - X'} \right|^{2m} \,. \tag{11}$$

In order to solve the eigenvalue problem, we take the Fourier transform of both sides of Eq. (11) and obtain:

$$\hat{Z}(k) = N\hat{L}_{\mu/2}^{C(E),\beta(E)}(k) \int dh \, dX' \, P(h) \left| \frac{h}{E - X'} \right|^{2m} Z(X') \, e^{-ikh^2/(E - X')} \,, \tag{12}$$

where $\hat{L}^{C(E),\beta(E)}_{\mu/2}(k)$ is the Fourier transform of the Lévy stable distribution:

$$\hat{L}_{\mu/2}^{C(E),\beta(E)}(k) = \exp\left[-C(E)|k|^{\mu/2} \left(1 + i\beta(E)\tan\left(\frac{\pi\mu}{4}\right)\operatorname{sign}(k)\right)\right]. \tag{13}$$

Using the fact that:

$$\int_0^\infty dx \, \frac{e^{ikx}}{x^a} = e^{i\frac{\pi}{2}(1-a)\operatorname{sign}(k)} |k|^{a-1} \Gamma(1-a) \,, \tag{14}$$

we can easily integrate over the disorder matrix element distribution obtaining:

$$\int_0^\infty \mathrm{d}h \, P(h) \, |h|^{2m} \, e^{-ikh^2/(E-X')} = \frac{1}{2N} \, \Gamma(m-\mu/2) \, e^{-i\frac{\pi}{2}(m-\mu/2)\mathrm{sign}(k(E-X'))} \, \left| \frac{k}{E-X'} \right|^{\mu/2-m} \, .$$

Plugging the result above into Eq. (12) we get:

$$\hat{Z}(k) = \frac{1}{2} \Gamma(m - \mu/2) |k|^{\mu/2 - m} \hat{L}_{\mu/2}^{C(E),\beta(E)}(k) \int_{-\infty}^{+\infty} dX' \frac{Z(X')}{|E - X'|^{m + \mu/2}} e^{-i\frac{\pi}{2}(m - \mu/2)\operatorname{sign}(k(E - X'))}.$$
 (15)

Note that this is exactly the same equation found in [1], where the authors studied the stability of the localized phase by determining the Lyapunov exponent of the imaginary part of the self-energy under iteration.

It is convenient to replace Z(X') by the inverse Fourier transform of $\hat{Z}(k')$. We then perform the integral over dX' by separating it into two pieces, and changing variable $E-S\to z$ in the interval $(-\infty,E)$ and $S-E\to z$ in the interval $(E,+\infty)$. Using again Eq. (14) we find:

$$\begin{split} & \int_{-\infty}^{+\infty} \mathrm{d}X' \, \frac{e^{ik'X'}}{|E-X'|^{m+\mu/2}} e^{-i\frac{\pi}{2}(m-\mu/2)\mathrm{sign}(k(E-X'))} = \\ & e^{ik'E} \, \Gamma(1-m-\mu/2) \, |k'|^{m+\mu/2-1} \left[e^{-i\frac{\pi}{2}(m-\mu/2)\mathrm{sign}(k)} \, e^{-i\frac{\pi}{2}(1-m-\mu/2)\mathrm{sign}(k')} + e^{i\frac{\pi}{2}(m-\mu/2)\mathrm{sign}(k)} \, e^{i\frac{\pi}{2}(1-m-\mu/2)\mathrm{sign}(k')} \right] \, . \end{split}$$

We plug back this last result into Eq. (15) and get:

$$\hat{Z}_{+}(k) = \frac{1}{2} \Gamma(m - \mu/2) \Gamma(1 - m - \mu/2) |k|^{\mu/2 - m} \hat{L}_{\mu/2}^{C(E),\beta(E)}(k) \left[\sin\left(\frac{\pi\mu}{2}\right) I_{+} + \sin\left(\pi m\right) I_{-} \right],$$

$$\hat{Z}_{-}(k) = \frac{1}{2} \Gamma(m - \mu/2) \Gamma(1 - m - \mu/2) |k|^{\mu/2 - m} \hat{L}_{\mu/2}^{C(E),\beta(E)}(k) \left[\sin\left(\pi m\right) I_{+} + \sin\left(\frac{\pi\mu}{2}\right) I_{-} \right],$$

where I_{+} and I_{-} are defined as:

$$I_{+} = \int_{0}^{+\infty} \frac{\mathrm{d}k'}{\pi} e^{ik'E} |k'|^{m+\mu/2-1} \hat{Z}(k'),$$

$$I_{-} = \int_{-\infty}^{0} \frac{\mathrm{d}k'}{\pi} e^{ik'E} |k'|^{m+\mu/2-1} \hat{Z}(k').$$

We also define $\hat{Z}_{+}(k)$ and $\hat{Z}_{-}(k)$ as the function $\hat{Z}(k)$ restricted to the regions k > 0 and k < 0 respectively, and introduce the coefficients:

$$K_{m,\mu} = \frac{1}{2} \Gamma \left(m - \frac{\mu}{2} \right) \Gamma \left(1 - m - \frac{\mu}{2} \right) ,$$

$$s_{\mu} = \sin \left(\frac{\pi \mu}{2} \right) ,$$

$$s_{m} = \sin \left(\pi m \right) ,$$

as done in the main text. We multiply both $\hat{Z}_{+}(k)$ and $\hat{Z}_{-}(k)$ by $e^{ikE} |k|^{m+\mu/2-1}$ and integrate them over dk/π in the intervals $(0, +\infty)$ and $(-\infty, 0)$ respectively. We then obtain:

$$I_{+} = K_{m,\mu} (s_{\mu}I_{+} + s_{m}I_{-}) \ell_{+},$$

$$I_{-} = K_{m,\mu} (s_{m}I_{+} + s_{\mu}I_{-}) \ell_{-},$$
(16)

where ℓ_+ and ℓ_- are defined as:

$$\ell_{+} = \int_{0}^{+\infty} \frac{\mathrm{d}k}{\pi} e^{ikE} |k|^{\mu-1} \hat{L}_{\mu/2}^{C(E),\beta(E)}(k) ,$$

$$\ell_{-} = \int_{-\infty}^{0} \frac{\mathrm{d}k}{\pi} e^{ikE} |k|^{\mu-1} \hat{L}_{\mu/2}^{C(E),\beta(E)}(k) .$$

The 2×2 linear system (16) only has non-trivial solutions different from zero if the determinant of the matrix of the coefficients vanishes. Hence the equation (10) for the mobility edge reads:

$$K_{m,\mu}^{2}\ell_{+}\ell_{-}\left[s_{\mu}^{2}-s_{m}^{2}\right]-K_{m,\mu}\left(\ell_{+}+\ell_{-}\right)s_{\mu}+1=0. \tag{17}$$

Using the specific form of $\hat{L}_{\mu/2}^{C(E),\beta(E)}(k)$, Eq. (13), it is straightforward to show that $\ell_- = \ell_+^*$. Interestingly enough, we remark that, as for the Anderson model on the Bethe lattice [6], the l.h.s. of Eq. (17) is a symmetric function of m around m = 1/2. This implies that, if a solution of Eq. (17) exists, then the stationary condition $\partial \lambda(m, E^*)/\partial m = 0$ can only be verified for m = 1/2. Hence, Eq. (17) finally becomes Eq. (2) of the main text.

We have solved Eq. (17)-together with Eqs. (6a) and Eqs. (6b)-numerically for several values of $\mu \in (0,1)$ and E (and for m = 1/2), and obtained the phase diagram of fig. 1 of the main text.

NUMERICAL RESULTS FOR $\mu \in (1, 2)$

In this section we provide several numerical results obtained from exact diagonalisations of Lévy Matrices in the range $\mu \in (1,2)$, for several system sizes $N=2^m$, with m from 8 to 14. As explained in the main text, the data are averaged over (at least) 2^{22-m} realization of the disorder. The energy spectrum is resolved in 64 small intervals ν , centered around the energies $E_{\nu} = \langle \lambda_n \rangle_{\nu}$.

In fig. 4 we plot q_{ν}^{typ} as a function of E_{ν} for $\mu=1.5$ and for different system sizes, averaged over samples and eigenstates within each energy window. Although at high energies our numerical data are still quite far from full convergence, it is clear that q_{ν}^{typ} evolve towards the GOE universal value, $q_{GOE}^{typ}=2/\pi$ in all energy windows as N is increased.

In fig. 5 we show the probability distribution of the gap ratio, $\Pi(r)$, for $\mu=1.5$, for different system sizes, and for four different values of the energy. In the case of Poisson statistics the probability distribution of the gap ratio is given by $\Pi(r)=2/(1+r)^2$, while the counterpart of $\Pi(r)$ corresponding to GOE statistics has been computed exactly in [8]. Level repulsion in the GOE spectra manifests itself in the vanishing of the probability distribution at r=0. As expected, at small enough energy the entire probability distribution $\Pi(r)$ is described by GOE. Finite size effects are stronger at higher energies. In particular for $E\simeq 9.99$ (bottom-right panel of 5), $\Pi(r)$ is still quite far from convergence even at the largest system size. Nevertheless it is clear that the distribution of the gap ratio is slowly evolving towards the GOE distribution as N is increased.

Numerical results on the Inverse Participation Ratios (IPR) are coherent with previous findings. The IPR of the eigen-function n is defined as: $\Upsilon_{2,n} = \sum_{i=1}^{N} |\langle i|n\rangle|^4$. In fig. 6 we plot the energy dependence of the exponent $\beta = \langle \ln \Upsilon_{2,n} \rangle_{\nu} / \ln N$ describing the scaling of the typical value of the IPR with the system size. At small enough energies we find $\beta \simeq 1$, corresponding to the standard scaling of the IPR for fully delocalized states. As mentioned

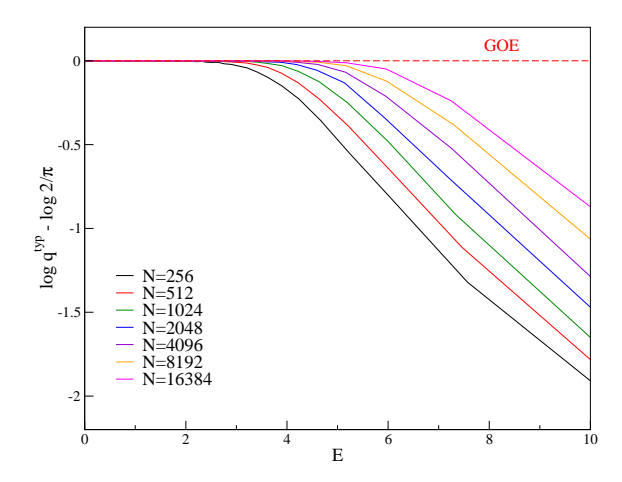


FIG. 4. $\ln(q^{typ}/q_{GOE}^{typ})$ as a function of the energy E for different system sizes for $\mu = 1.5$.

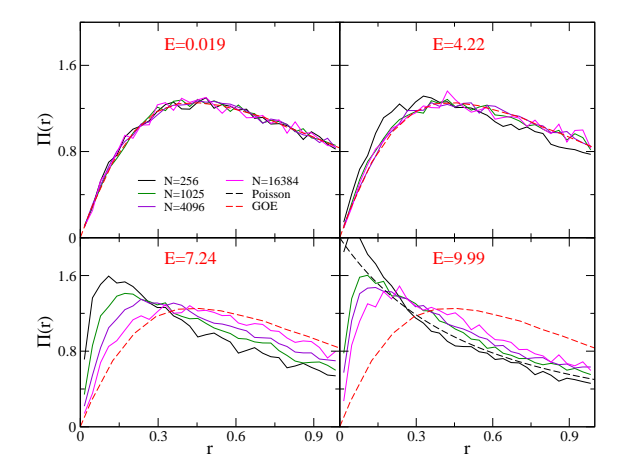


FIG. 5. Probability distribution of the gap ratio for $\mu=1.5$, for different system sizes, and for four different values of the energy. The Poisson and GOE counterparts of $\Pi(r)$ are also shown. Top-left panel: E=0.019; The entire probability distribution is described by the GOE. Top-right panel: E=4.22; $\Pi(r)$ converges to the GOE distribution for N large enough. Bottom-left panel: E=7.24; $\Pi(r)$ evolves towards the GOE distribution as N is increased, although we are not able to observe full convergence. Bottom-right panel: E=9.99; $\Pi(r)$ is very far from convergence even for the largest system size considered, although it slowly evolves towards the GOE distribution.

above, finite size effects are stronger at higher energies. We indeed observe that β decreases as the energy grows for a fixed system size N. Nevertheless, at fixed energy, β increases as the system size is increased and seems to approach the standard value 1 in all energy windows. This is confirmed by the numerical results on the the support set, recently introduced in [9] as a tough measure wave-functions ergodicity. For an eigenvector n with sites ordered according to $|\langle i|n\rangle| > |\langle i+1|n\rangle|$, it is defined as the sets of sites $i < S_{\epsilon}^{(n)}$ such that $\sum_{i=1}^{S_{\epsilon}^{(n)}} |\langle i|n\rangle|^2 \le 1 - \epsilon < \sum_{i=1}^{S_{\epsilon}^{(n)}+1} |\langle i|n\rangle|^2$. The scaling of $\langle S_{\epsilon}^{(n)} \rangle$ for $N \to \infty$ and ϵ arbitrary small but finite allows to discriminate between the extended and the localized regimes, as $S_{\epsilon}^{(n)}$ is N-independent for localized wave-functions while it diverges for $N \to \infty$ for delocalized states. The exponent $\beta' = \ln \langle S_{\epsilon}^{(n)} \rangle_{\nu} / \ln N$, describing the scaling of the support set at large N is also shown in fig. 6. Its behavior is very similar to the one of β described above. However the support set is apparently a sharper measure of wave-functions ergodicity compared to the IPR, as the values of β' are much closer to 1 in all energy windows.

Similar results are obtained for $\mu = 1.1$, confirming that for $\mu \in (1,2)$ all eigenstates of LMs are extended and the level statistics is described by GOE in the whole spectrum. Nevertheless finite size effect become stronger as μ is lowered and can be extremely important at high energies, where one needs to consider relatively large N to observe full converges towards GOE.

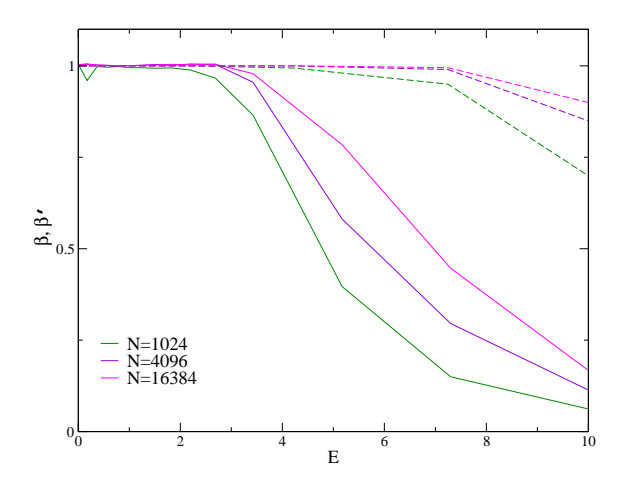


FIG. 6. Exponents β (continuous lines) and β' (dashed lines) describing the scaling with N of the typical value of the Inverse Participation Ratio and of the support set as a function of the energy for $\mu = 1.5$.

NUMERICAL RESULTS FOR $\mu \in (0,1)$

According to the expression (3) of the probability distribution of the entries of our LMs, each row (or column) of \mathcal{H} has O(N) elements of $O(N^{-1/\mu})$ and O(1) elements of O(1), ensuring a well-defined thermodynamic limit. However, a simple calculation shows that the largest element of the whole matrix (which contains N^2 terms) is of order $N^{1/\mu}$. As a consequence, for large enough system sizes and for $\mu < 1$, the range of variability of the matrix elements is extremely broad, from $O(N^{-1/\mu})$ to $O(N^{1/\mu})$. This could affect the numerical precisions of our results. In order to overcome this issue, we have introduced a cut-off on large matrix elements scaling as $\Lambda N^{1/\mu}$, where Λ is a constant much larger than 1. Since we are only interested in the properties of LMs for energies of O(1), the presence of such cut-off does not have any influence on our numerical results (provided that Λ is large enough).

Furthermore, in order to exploit the "sparse-like" character of LMs, we introduce a cut-off γ (very small but finite) on small matrix elements which allows to transform \mathcal{H} in a sparse Erdös-Rényi random matrix constituted by the backbone of large entries [10]. This allows to simplify and speed-up the numerical calculations, since numerical routines for exact diagonalisation are faster for sparse matrices. The probability distributions of the entry thus becomes:

$$P_N^{(\gamma,\Lambda)}(h_{ij}) = p_N^{(\gamma)} \delta(h_{ij}) + (1 - p_N^{(\gamma)}) \theta \left(\gamma < |h_{ij}| < N\Lambda \right) \frac{C_N^{(\gamma,\Lambda)}}{2|h_{ij}|^{1+\mu}} ,$$

where
$$p_N^{(\gamma)} = 1 - 1/(N\mu\gamma^{\mu})$$
 and $C_N^{(\gamma,\Lambda)} = \mu/[\gamma^{-\mu} - (N\Lambda)^{-\mu}].$

where $p_N^{(\gamma)}=1-1/(N\mu\gamma^\mu)$ and $C_N^{(\gamma,\Lambda)}=\mu/[\gamma^{-\mu}-(N\Lambda)^{-\mu}]$. We have performed exact diagonalisations of such random matrices for several system sizes $N=2^m$, with m from 8 to 15, and for $\Lambda=2^{15}$. Data are averaged over (at least) 2^{22-m} realization of the disorder. The energy spectrum is resolved in 64 small intervals ν , centered around the energies $E_{\nu} = \langle \lambda_n \rangle_{\nu}$. In order to make sure that the cut-off on small entries is small enough to reproduce the $\gamma \to 0$ limit, we have considered different values of γ ($\gamma = 10^{-3}$, 10^{-4} , and $5 \cdot 10^{-5}$) and checked that the data become independent of it (within our numerical accuracy).

In the following we complement the discussion of the main text with more details and results obtained from exact diagonalisations for $\mu \in (0,1)$. We will focus more specifically on $\mu = 0.5$. Similar results are found for $\mu = 0.8$ and $\mu = 0.3$, although finite size effects becomes bigger as μ is decreased and the crossover region gets broader.

In fig. 7 we plot q_{ν}^{typ} as a function of E_{ν} for $\mu = 0.5$ and for different system sizes, averaged over samples and eigenstates within each energy window. For small (resp. large) energies we recover, as expected, the universal values $q_P^{typ} = 2/\pi$ (resp. $q_P^{typ} \to 0$) corresponding to GOE (resp. Poisson) statistics. As mentioned in the main text, the curves corresponding to different values of N seem to cross much before the localization transition, which can be computed analytically and should occur at $E^* \simeq 15.4$. However, our numerical data on q^{typ} are extremely clean and allow to observe that the crossing point is actually slowly drifting towards higher values of the energy (and most probably converging to E^* in the thermodynamic limit).

In fig. 8, we show the probability distribution of the gap ratio, $\Pi(r)$, for $\mu = 0.5$, for different system sizes, and for four different values of the energy. As expected, for small enough energies (e.g., $E \simeq 0.063$, top-left panel) the entire probability distribution is described by GOE statistics. Conversely, for high enough energies (e.g., $E \simeq 30.71$,

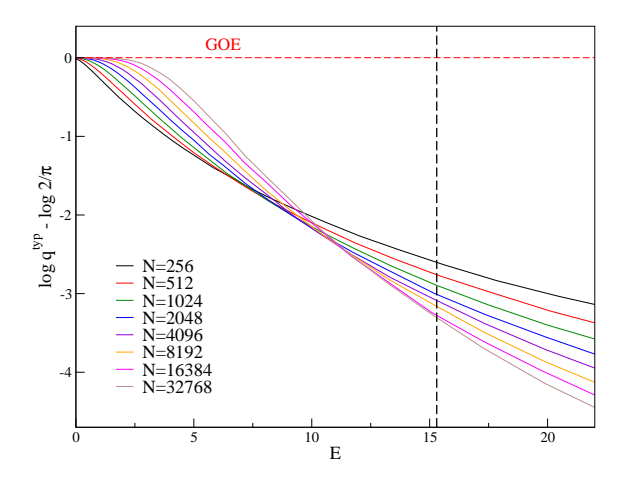


FIG. 7. $\ln(q^{typ}/q_{GOE}^{typ})$ as a function of the energy E for different system sizes for $\mu = 0.5$.

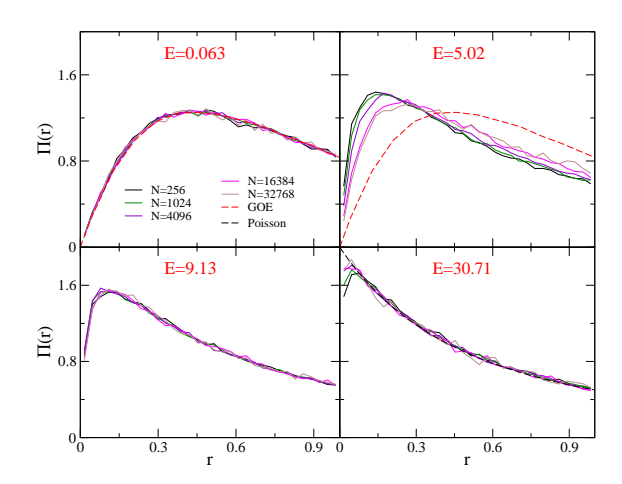


FIG. 8. Probability distribution of the gap ratio for $\mu=0.5$, for different system sizes, and for four different values of the energy. The Poisson and GOE counterparts of $\Pi(r)$ are also shown. Top-left panel: E=0.063; The entire probability distribution is described by the GOE. Top-right panel: E=5.02; $\Pi(r)$ evolves towards the GOE distribution as N is increased, although we are not able to observe full convergence. Bottom-left panel: E=9.13; $\Pi(r)$ seems to be described by a N-independent non-unversal distribution. Bottom-right panel: E=30.71; $\Pi(r)$ converges to the Poisson distribution for large N.

bottom-right panel), in the localized regime, the data nicely approach the Poisson distribution $\Pi(r) = 2/(1+r)^2-$ except for very small values of r where convergence is exponentially slow due to finite size effects. For moderately high energies (e.g., E = 5.02, top-right panel), $\Pi(r)$ evolves towards the GOE distribution as N is increased, although we are not able to observe full convergence for the largest system size. Finally, for energies in the crossover region (e.g., E = 9.13, bottom-left panel), one seems to observe that $\Pi(r)$ is described by a stationary (i.e., N-independent) and non-universal-neither GOE nor Poisson-distribution, as observed in [1]. Nevertheless, if one analyzes carefully the numerical data, focusing, for instance, on the behavior of $\Pi(r)$ at small r, one realizes that $\Pi(r)$ evolves in a non-monotonic way: for system sizes smaller than the crossover size, $N < N_m \simeq 1200$ (see the inset of fig. 3 of the main text), it evolves towards the Poisson distribution, while for large system sizes, $N > N_m$, it commences to approach the GOE distribution. However, it is evident that if one ignored the existence of the crossover scale, based on the bottom-left panel of fig. 8 one would certainly conclude that for intermediate energies a new and non-universal "mixed" level statistics is found.

In fig. 9 we plot the energy dependence of the exponents $\beta = \langle \ln \Upsilon_{2,n} \rangle_{\nu} / \ln N$ and $\beta' = \ln \langle S_{\epsilon}^{(n)} \rangle_{\nu} / \ln N$ describing the scaling with the system size of the typical value of the IPR and of the average support set respectively, for $\mu = 0.5$. The behavior of β and β' is coherent with previous results, at least for sufficiently small and sufficiently large energies. More precisely, one observes that, at fixed N, β and β' decrease as the energy is increased. Nevertheless, at fixed and small enough energy, they both grow with N and seem to approach the standard value 1 for $N \to \infty$. Conversely, at fixed and large enough energy, in the localized regime, β and β' decrease to zero as the system size is increased,

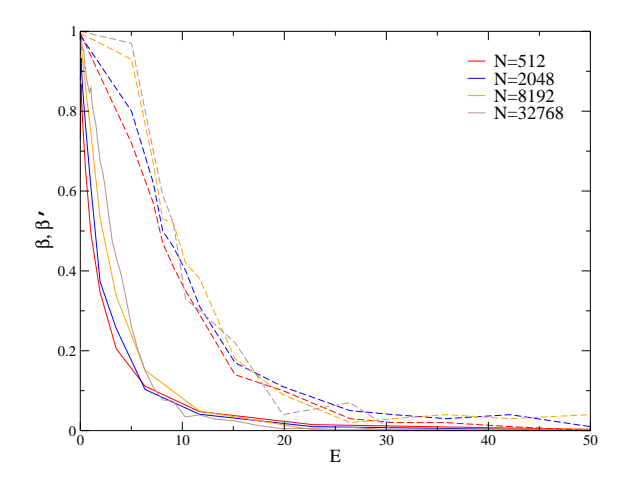


FIG. 9. Exponents β (continuous lines) and β' (dashed lines) describing the scaling with N of the typical value of the Inverse Participation Ratio and of the support set as a function of the energy for $\mu = 0.5$.

implying that $\langle \Upsilon_{2,n} \rangle_{\nu}, \langle S_{\epsilon}^{(n)} \rangle_{\nu} \to \text{cst.}$ As mentioned above, the support set provides a more precise measure of wavefunction ergodicity compared to the IPR. In particular, the exponent β is much smaller than one already very far from the localization transition. In the crossover region one should expect that β and β' show a non-monotonic behavior as a function of N on the crossover scale $N_m(E)$. However, our numerical data are too noisy to capture this behavior. In fact, numerics based solely on the IPRs are inconclusive and could be undoubtedly misinterpreted, especially for intermediate energies within the crossover regime, since they are affected by strong finite size effects.

NUMERICAL SOLUTION OF THE SELF-CONSISTENT EQUATION FOR Q(G)

In this section we provide more details on the numerical solutions of the self-consistent equation on the probability distribution of the diagonal elements of the resolvent matrix.

In order to device an accurate and efficient algorithm to compute Q(G) it is convenient to make use, again, of the "sparse-like" character of LMs [10]. As explained above, each row (or column) of \mathcal{H} has O(N) elements of $O(N^{-1/\mu})$ and O(1) elements of O(1). We thus introduce a cut-off γ that separates large matrix elements $(|h_{ij}| > \gamma)$ from small ones $(|h_{ij}| < \gamma)$. The backbone of large entries constitutes thus a sparse (Erdös-Rényi) RM, with average connectivity $c_{\gamma} = 2N \int_{\gamma}^{\infty} P(h) dh = 1/(\mu \gamma^{\mu})$ [11]. Since the probability distribution of small matrix elements has now a finite variance $\sigma_{\gamma}^2 = 2 \int_{(N\mu)^{-1/\mu}}^{\gamma} h^2 P(h) dh = \gamma^{2-\mu}/[N(2-\mu)]$, their contribution to the sum in Eq. (1) of the main text can be handled using the (classical) central limit theorem, yielding the following self-consistent equation for $Q_{\gamma}(G)$ (in the limit $\gamma \to 0$):

$$Q_{\gamma}(G) = \sum_{k=0}^{\infty} p_{\gamma}(k) \int \prod_{i=1}^{k} \left[dG_i Q_{\gamma}(G_i) dh_i P(h_i) \right] \delta \left(G^{-1} - E + i\eta + \sigma_{\gamma}^2 \langle G \rangle + \sum_{i=0}^{k} h_i^2 G_i \right), \tag{18}$$

where $p_{\gamma}(k) = e^{-c_{\gamma}} c_{\gamma}^{k}/k!$ is the Poisson distribution of the connectivity. This equation can be efficiently solved using a population dynamics algorithm [12]. We have used a population of 2^{26} elements, and computed $Q_{\gamma}(G)$ for $\gamma = 10^{-3}, 10^{-4}, 5 \cdot 10^{-5}$, and extrapolated the results for $\gamma \to 0$.

In fig. 10 we show the marginal probability distribution of $\ln \mathrm{Im} G_{ii}$ for several values of the imaginary regulator η and for E=5, deep in the GOE ergodic phase. Since the system is delocalized and the spectrum is absolutely continuous, $\tilde{Q}_I(\ln \mathrm{Im} G)$ must have a non-singular limit as $\eta \to 0^+$. We indeed observe a stationary η -independent distribution for η sufficiently small ($\eta \lesssim 10^{-6}$). As a consequence, $\langle \Upsilon_2 \rangle \to 0$ for $\eta \to 0^+$.

Conversely, in the localized phase the marginal probability distribution of the imaginary part of G_{ii} has a singular behavior as $\eta \to 0^+$, as illustrated in fig. 11. Almost all values of $\text{Im}G_{ii}$ are of order η , except extremely rare events—whose fraction vanishes as η —described by heavy power-law tails with an exponent 1+m and m=1/2. More precisely, $\tilde{Q}_I(\text{Im}G)$ has a scaling form $f(x/\eta)\eta$ for $x \sim \eta$, with $\int f(y) dy = 1$, and fat tails

$$\tilde{Q}_I(\text{Im}G) \simeq \frac{c \,\eta^{1-m}}{(\text{Im}G)^{1+m}} \,, \tag{19}$$

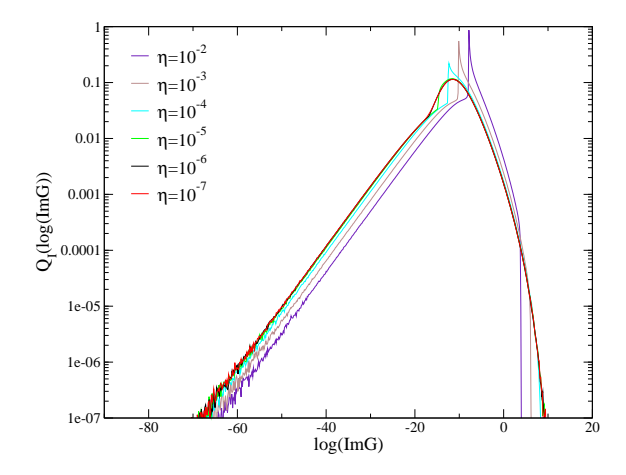


FIG. 10. Marginal probability distribution of $\ln \operatorname{Im} G$ for different values of the imaginary regulator η and for E=5, showing convergence to a stationary η -independent distribution for small enough η .

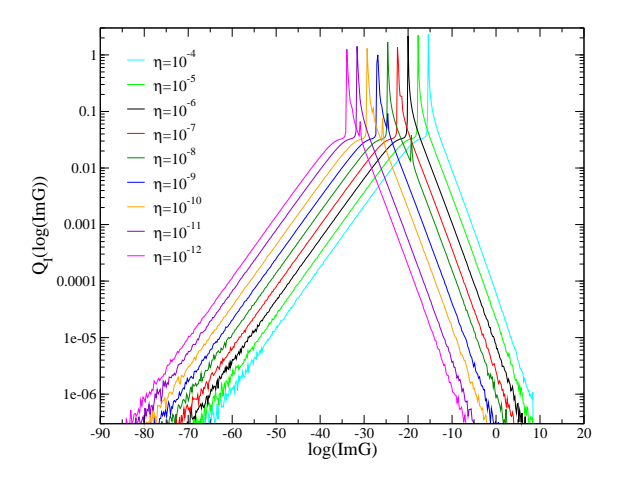


FIG. 11. Marginal probability distribution of $\ln \operatorname{Im} G$ for different values of the imaginary regulator η and for E=22. In the localized phase the limit $\eta \to 0^+$ is singular: Almost all values of $\operatorname{Im} G_{ii}$ are of order η , except extremely rare events described by heavy power-law tails with an exponent 1+m=3/2 whose coefficient vanishing as $\sqrt{\eta}$.

with c being a constant of O(1), and a cut-off for $\text{Im}G_{ii} \simeq 1/\eta$. Such tails gives a contribution of O(1) to the density of states, whereas the bulk part only yields a vanishing contribution. The marginal probability distribution of the real part of G_{ii} (not shown) converges to a stationary distribution with power-law tails with a E-independent exponent 1 + m = 2. This implies that in the localized phase $\langle \Upsilon_2 \rangle \to \text{cst for } \eta \to 0^+$.

In fig. 12 we show the behavior of $\tilde{Q}_I(\ln {\rm Im}G)$ in the crossover region. Since the system is delocalized, we know that the $\eta \to 0^+$ limit exists and is non-singular. However, convergence to a stationary distribution is observed only for extremely small values of the imaginary regulator, $\eta \lesssim 10^{-13}$ in this case. For η small enough but still larger than 10^{-13} , one observes that, similarly to the localized regime, the marginal distribution of ${\rm Im}G_{ii}$ displays "singular" power-law tails described by $\tilde{Q}_I({\rm Im}G) \sim \eta^{1-m}/({\rm Im}G)^{1+m}$ with an exponent $1/2 \lesssim m < 1$, and a cut-off for ${\rm Im}G_{ii} \simeq 1/\eta$ (the exponent is instead $m \simeq 1$ for the marginal distribution of ${\rm Re}G_{ii}$). This implies that for large enough η the tails of $\tilde{Q}_I(\ln {\rm Im}G)$ give a O(1) contribution to the density of states, whereas the bulk part gives a contribution of $O(\eta)$, as if the system was non-ergodic.

In order to extract the crossover scale $N'_m(E)$, we measure the typical value of the imaginary part of G_{ii} , $\operatorname{Im} G_{ii}^{typ} = e^{\langle \ln \operatorname{Im} G_{ii} \rangle}$, over the stationary distribution on the localized phase and, following the argument presented in the main text, we define $N'_m(E) = 1/(\operatorname{Im} G_{ii}^{typ} \rho(E))$. In fig. 13 we plot $\ln N'_m(E)$ as a function of $\ln N_m(E)$, showing a linear relation between these two quantities. This implies that our argument allows to capture correctly the origin of finite size effects.

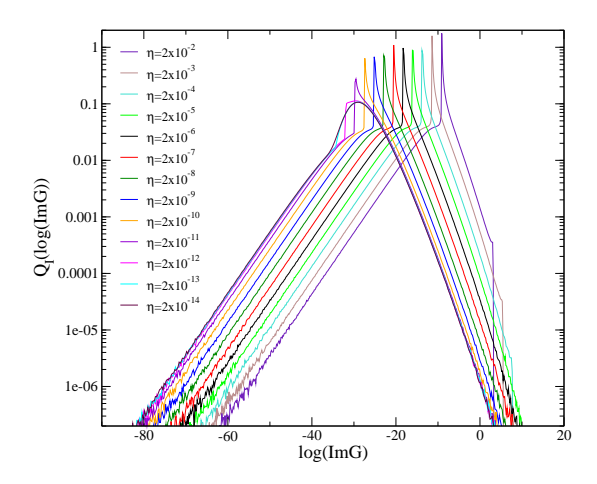


FIG. 12. Marginal probability distribution of $\ln \operatorname{Im} G$ for different values of the imaginary regulator η and for E=13, in the crossover phase. For $\eta>10^{13}$ the system behaves as it was localized and non ergodic, showing "singular" power-law tails with an exponent 1+m with $1/2 \lesssim m < 1$ and a cut-off in $\operatorname{Im} G=1/\eta$. Convergence to a stationary non-singular distribution is achieved for $\eta<10^{13}$.

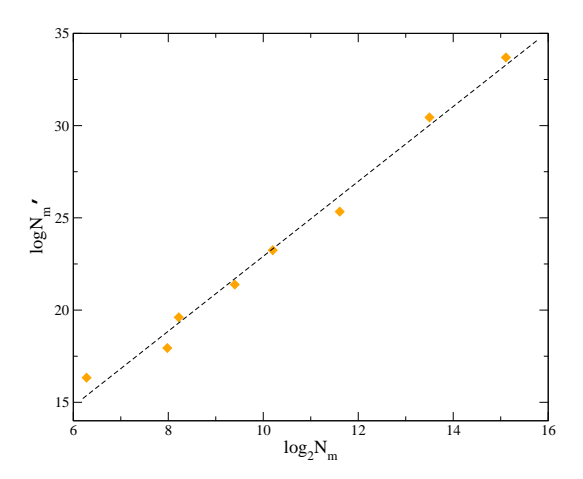


FIG. 13. $\ln N'_m(E)$ as a function of $\ln N_m(E)$.

- [1] P. Cizeau and J.-P. Bouchaud, Phys. Rev. E **50**, 1810 (1994).
- [2] G. Ben Arous and A. Guionnet, Comm. in Math. Phys. 278 715 (2008).
- [3] B. Derrida and H. Spohn, J. Stat. Phys. **51**, 817 (1988).
- [4] B. Derrida, Phys. Rev. Lett. 45, 79 (1980).
- [5] M. Aizenman and S. Warzel, J. of the Europ. Math. Soc. 15 1167 (2013).
- [6] R. Abou-Chacra, P.W. Anderson, and D.J. Thouless, J. Phys. C: Solid St. Phys. 6, 1734 (1973).
- [7] V. Bapst, J. Math. Phys. **55**, 092101 (2014).
- [8] Y.Y. Atas, E. Bogomolny, O. Giraud, and P. Vivo, J. Phys. A: Math. Gen. 46, 355204 (2103).
- [9] A. De Luca, V.E. Kravtsov, B. L. Altshuler, and A. Scardicchio arXiv:1401.0019.
- [10] F.L. Metz, I. Neri, and D Bollé, Phys. Rev. E 82, 031135 (2010).
- [11] K. Janzen, A. Engel, and M. Mézard, Europhys. Lett. 89, 67002 (2010).
- [12] M. Mézard and G. Parisi, Eur. Phys. J. B 20 (2001), 217.